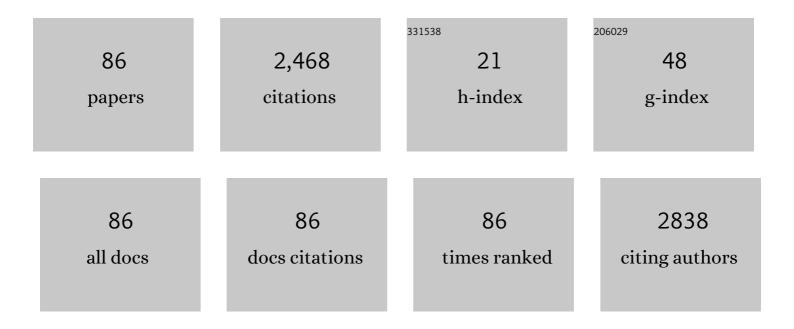
Azat G Gabdulkhakov

List of Publications by Year in descending order

Source: https://exaly.com/author-pdf/7667940/publications.pdf Version: 2024-02-01



#	Article	IF	CITATIONS
1	Cyanobacterial photosystem II at 2.9-Ã resolution and the role of quinones, lipids, channels and chloride. Nature Structural and Molecular Biology, 2009, 16, 334-342.	3.6	1,105
2	Probing the Accessibility of the Mn4Ca Cluster in Photosystem II: Channels Calculation, Noble Gas Derivatization, and Cocrystallization with DMSO. Structure, 2009, 17, 1223-1234.	1.6	120
3	Recent Progress in the Crystallographic Studies of Photosystem II. ChemPhysChem, 2010, 11, 1160-1171.	1.0	102
4	Crystal structure of a mirror-image L-RNA aptamer (Spiegelmer) in complex with the natural L-protein target CCL2. Nature Communications, 2015, 6, 6923.	5.8	77
5	Structural Basis of Cyanobacterial Photosystem II Inhibition by the Herbicide Terbutryn. Journal of Biological Chemistry, 2011, 286, 15964-15972.	1.6	73
6	Structural insights into the catalytic mechanism of sphingomyelinases D and evolutionary relationship to glycerophosphodiester phosphodiesterases. Biochemical and Biophysical Research Communications, 2006, 342, 323-329.	1.0	63
7	Crystal Structure of Monomeric Photosystem II from Thermosynechococcus elongatus at 3.6-Ã Resolution. Journal of Biological Chemistry, 2010, 285, 26255-26262.	1.6	62
8	Ribosomal protein L1 recognizes the same specific structural motif in its target sites on the autoregulatory mRNA and 23S rRNA. Nucleic Acids Research, 2005, 33, 478-485.	6.5	56
9	X-ray structural studies of the fungal laccase from Cerrena maxima. Journal of Biological Inorganic Chemistry, 2006, 11, 963-973.	1.1	47
10	Structural and functional characterization of two-domain laccase from Streptomyces viridochromogenes. Biochimie, 2015, 112, 151-159.	1.3	42
11	Double Suppression of the Cα Protein Activity by RGS Proteins. Molecular Cell, 2014, 53, 663-671.	4.5	40
12	Revisiting the <i>Haloarcula marismortui</i> 50S ribosomal subunit model. Acta Crystallographica Section D: Biological Crystallography, 2013, 69, 997-1004.	2.5	40
13	Structure of the polypeptide crotamine from the Brazilian rattlesnake <i>Crotalus durissus terrificus</i> . Acta Crystallographica Section D: Biological Crystallography, 2013, 69, 1958-1964.	2.5	37
14	Three-Dimensional Structure of N-Terminal Domain of DnaB Helicase and Helicase-Primase Interactions in Helicobacter pylori. PLoS ONE, 2009, 4, e7515.	1.1	34
15	Mechanism of ribosome shutdown by RsfS in Staphylococcus aureus revealed by integrative structural biology approach. Nature Communications, 2020, 11, 1656.	5.8	30
16	Purification, crystallization and preliminary X-ray study of the fungal laccase fromCerrena maxima. Acta Crystallographica Section F: Structural Biology Communications, 2006, 62, 954-957.	0.7	27
17	High-resolution crystal structure of the isolated ribosomal L1 stalk. Acta Crystallographica Section D: Biological Crystallography, 2012, 68, 1051-1057.	2.5	26
18	The structures of mutant forms of Hfq from <i>Pseudomonas aeruginosa</i> reveal the importance of the conserved His57 for the protein hexamer organization. Acta Crystallographica Section F: Structural Biology Communications, 2010, 66, 760-764.	0.7	25

#	Article	IF	CITATIONS
19	Mistletoe lectin I in complex with galactose and lactose reveals distinct sugar-binding properties. Acta Crystallographica Section F: Structural Biology Communications, 2005, 61, 17-25.	0.7	22
20	Insights into metal ion binding inÂphospholipases A2: ultra high-resolution crystal structures ofÂanÂacidic phospholipase A2 inÂtheÂCa2+ free andÂbound states. Biochimie, 2006, 88, 543-549.	1.3	22
21	Asp49 phospholipase A2–elaidoylamide complex: a new mode of inhibition. Biochemical and Biophysical Research Communications, 2004, 319, 1314-1321.	1.0	21
22	Preliminary investigation of the three-dimensional structure ofSalmonella typhimuriumuridine phosphorylase in the crystalline state. Acta Crystallographica Section F: Structural Biology Communications, 2005, 61, 337-340.	0.7	18
23	The X-ray structure ofSalmonella typhimuriumuridine nucleoside phosphorylase complexed with 2,2′-anhydrouridine, phosphate and potassium ions at 1.86â€Ã resolution. Acta Crystallographica Section D: Biological Crystallography, 2010, 66, 51-60.	2.5	18
24	Investigations of Accessibility of T2/T3 Copper Center of Two-Domain Laccase from Streptomyces griseoflavus Ac-993. International Journal of Molecular Sciences, 2019, 20, 3184.	1.8	18
25	Controlling Photosynthetic Excitons by Selective Pigment Photooxidation. Journal of Physical Chemistry B, 2019, 123, 29-38.	1.2	18
26	Three-dimensional structure of laccase from Coriolus zonatus at 2.6 Ã resolution. Crystallography Reports, 2006, 51, 817-823.	0.1	15
27	Binding of the 5′-Triphosphate End of mRNA to the γ-Subunit of Translation Initiation Factor 2 of the Crenarchaeon Sulfolobus solfataricus. Journal of Molecular Biology, 2015, 427, 3086-3095.	2.0	15
28	Purification, crystallization and preliminary X-ray diffraction analysis of crotamine, a myotoxic polypeptide from the Brazilian snakeCrotalus durissus terrificus. Acta Crystallographica Section F: Structural Biology Communications, 2012, 68, 1052-1054.	0.7	14
29	Cryoâ€EM structure of the ribosome functional complex of the human pathogen <i>StaphylococcusÂaureus</i> at 3.2ÂÃ resolution. FEBS Letters, 2020, 594, 3551-3567.	1.3	14
30	High-Resolution Crystal Structure of Spectrin SH3 Domain Fused with a Proline-Rich Peptide. Journal of Biomolecular Structure and Dynamics, 2011, 29, 485-495.	2.0	13
31	Protein–RNA affinity of ribosomal protein L1 mutants does not correlate with the number of intermolecular interactions. Acta Crystallographica Section D: Biological Crystallography, 2015, 71, 376-386.	2.5	12
32	Purification, crystallization and preliminary X-ray analysis of uridine phosphorylase fromSalmonella typhimurium. Acta Crystallographica Section D: Biological Crystallography, 2004, 60, 709-711.	2.5	11
33	Structural Studies of Component of Lysoamidase Bacteriolytic Complex from Lysobacter sp. XL1. Protein Journal, 2016, 35, 44-50.	0.7	10
34	Uridine phosphorylase in biomedical, structural, and functional aspects: A review. Crystallography Reports, 2011, 56, 560-589.	0.1	9
35	Molecular dynamics studies of pathways of water movement in cyanobacterial photosystem II. Crystallography Reports, 2015, 60, 83-89.	0.1	9
36	Crystal Structure of the 23S rRNA Fragment Specific to r-Protein L1 and Designed Model of the Ribosomal L1 Stalk from Haloarcula marismortui. Crystals, 2017, 7, 37.	1.0	9

#	Article	IF	CITATIONS
37	Engineering the Catalytic Properties of Two-Domain Laccase from Streptomyces griseoflavus Ac-993. International Journal of Molecular Sciences, 2022, 23, 65.	1.8	9
38	Structural and thermodynamic studies of Bergerac-SH3 chimeras. Biophysical Chemistry, 2009, 139, 106-115.	1.5	7
39	Comparative analysis of three-dimensional structures of homodimers of uridine phosphorylase from Salmonella typhimurium in the unligated state and in a complex with potassium ion. Crystallography Reports, 2009, 54, 267-278.	0.1	7
40	Purification, crystallization and preliminary X-ray structure analysis of the laccase from <i>Ganoderma lucidum</i> . Acta Crystallographica Section F: Structural Biology Communications, 2011, 67, 926-929.	0.7	7
41	X-ray structure ofSalmonella typhimuriumuridine phosphorylase complexed with 5-fluorouracil and molecular modelling of the complex of 5-fluorouracil with uridine phosphorylase fromVibrio cholerae. Acta Crystallographica Section D: Biological Crystallography, 2012, 68, 968-974.	2.5	7
42	Crystallization and X-ray diffraction studies of a two-domain laccase from <i>Streptomyces griseoflavus</i> . Acta Crystallographica Section F, Structural Biology Communications, 2015, 71, 1200-1204.	0.4	7
43	Analysis of molecular oxygen exit pathways in cyanobacterial photosystem II: Molecular dynamics studies. Crystallography Reports, 2015, 60, 884-888.	0.1	7
44	Topology of the polypeptide chain in the complex of agglutinin from castor bean seeds with β-D-galactose in the crystalline state. Crystallography Reports, 2001, 46, 792-800.	0.1	6
45	Crystal structure of ribosomal protein L1 from the bacterium Aquifex aeolicus. Crystallography Reports, 2011, 56, 603-607.	0.1	6
46	Structural analysis of interdomain mobility in ribosomal L1 proteins. Acta Crystallographica Section D: Biological Crystallography, 2011, 67, 1023-1027.	2.5	6
47	Expression, purification, crystallization and preliminary X-ray structure analysis ofVibrio choleraeuridine phosphorylase in complex with thymidine. Acta Crystallographica Section F: Structural Biology Communications, 2012, 68, 1394-1397.	0.7	6
48	Structural studies on photosystem II of cyanobacteria. Biochemistry (Moscow), 2013, 78, 1524-1538.	0.7	6
49	Crystallization and preliminary X-ray study ofVibrio choleraeuridine phosphorylase in complex with 6-methyluracil. Acta Crystallographica Section F, Structural Biology Communications, 2014, 70, 60-63.	0.4	6
50	Fab Fragment of VHH-Based Antibody Netakimab: Crystal Structure and Modeling Interaction with Cytokine IL-17A. Crystals, 2019, 9, 177.	1.0	6
51	Novel approaches for the lipid sponge phase crystallization of the <i>Rhodobacter sphaeroides</i> photosynthetic reaction center. IUCrJ, 2020, 7, 1084-1091.	1.0	6
52	Isolation, crystallization and preliminary crystallographic analysis ofSalmonella typhimuriumuridine phosphorylase crystallized with 2,2′-anhydrouridine. Acta Crystallographica Section F: Structural Biology Communications, 2007, 63, 852-854.	0.7	5
53	Structural basis for the mechanism of inhibition of uridine phosphorylase from Salmonella typhimurium. Crystallography Reports, 2010, 55, 41-57.	0.1	5
54	Expression, purification, crystallization and preliminary X-ray structure analysis of wild-type and L(M196)H-mutantRhodobacter sphaeroidesreaction centres. Acta Crystallographica Section F: Structural Biology Communications, 2013, 69, 506-509.	0.7	5

#	Article	IF	CITATIONS
55	Structural investigation of the thymidine phosphorylase from <i>Salmonella typhimurium</i> in the unliganded state and its complexes with thymidine and uridine. Acta Crystallographica Section F, Structural Biology Communications, 2016, 72, 224-233.	0.4	5
56	Structural and functional properties of antimicrobial protein L5 of Lysоbacter sp. XL1. Applied Microbiology and Biotechnology, 2018, 102, 10043-10053.	1.7	5
57	X-ray structure of the <i>Rhodobacter sphaeroides</i> reaction center with an M197 Phe→His substitution clarifies the properties of the mutant complex. IUCrJ, 2022, 9, 261-271.	1.0	5
58	Crystallization and preliminary X-ray diffraction analysis ofSalmonella typhimuriumuridine phosphorylase complexed with 5-fluorouracil. Acta Crystallographica Section F: Structural Biology Communications, 2009, 65, 601-603.	0.7	4
59	Different effects of identical symmetry-related mutations near the bacteriochlorophyll dimer in the photosynthetic reaction center of Rhodobacter sphaeroides. Biochemistry (Moscow), 2015, 80, 647-653.	0.7	4
60	Investigation of structure of the ribosomal L12/P stalk. Biochemistry (Moscow), 2016, 81, 1589-1601.	0.7	4
61	X-ray structures of uridine phosphorylase from Vibrio cholerae in complexes with uridine, thymidine, uracil, thymine, and phosphate anion: Substrate specificity of bacterial uridine phosphorylases. Crystallography Reports, 2016, 61, 954-973.	0.1	4
62	Dimerization of long hibernation promoting factor from Staphylococcus aureus: Structural analysis and biochemical characterization. Journal of Structural Biology, 2020, 209, 107408.	1.3	4
63	Structure of the ribosomal P stalk base in archaean Methanococcus jannaschii. Journal of Structural Biology, 2020, 211, 107559.	1.3	4
64	Crystallization and preliminary X-ray diffraction studies ofDrosophila melanogasterGαo-subunit of heterotrimeric G protein in complex with the RGS domain of CG5036. Acta Crystallographica Section F: Structural Biology Communications, 2013, 69, 61-64.	0.7	3
65	Structural and preliminary molecular dynamics studies of the Rhodobacter sphaeroides reaction center and its mutant form L(M196)H + H(M202)L. Crystallography Reports, 2014, 59, 536-541.	0.1	3
66	The L(M196)H mutation in Rhodobacter sphaeroides reaction center results in new electrostatic interactions. Photosynthesis Research, 2015, 125, 23-29.	1.6	3
67	Substrate specificity of pyrimidine nucleoside phosphorylases of NP-II family probed by X-ray crystallography and molecular modeling. Crystallography Reports, 2016, 61, 830-841.	0.1	3
68	Investigations of Photosensitive Proteins by Serial Crystallography. Biochemistry (Moscow), 2018, 83, S163-S175.	0.7	3
69	Serine bacteriolytic protease L1 of Lysobacter sp. XL1 complexed with protease inhibitor AEBSF: features of interaction. Process Biochemistry, 2019, 80, 89-94.	1.8	3
70	X-Ray Structure and Molecular Dynamics Study of Uridine Phosphorylase from Vibrio cholerae in Complex with 2,2'-Anhydrouridine. Crystallography Reports, 2020, 65, 269-277.	0.1	3
71	A preliminary X-ray diffraction study of the laccase from Coriolus zonatus in the native state. Crystallography Reports, 2006, 51, 278-285.	0.1	2
72	Structure of the homodimer of uridine phosphorylase from Salmonella typhimurium in the native state at 1.9 Ã resolution. Crystallography Reports, 2007, 52, 1072-1078.	0.1	2

Azat G Gabdulkhakov

#	Article	IF	CITATIONS
73	Crystallization of the two-domain N-terminal fragment of the archaeal ribosomal protein L10(P0) in complex with a specific fragment of 23S rRNA. Crystallography Reports, 2011, 56, 702-704.	0.1	2
74	Three-dimensional structure of photosystem II from Thermosynechococcus elongates in complex with terbutryn. Crystallography Reports, 2011, 56, 1054-1059.	0.1	2
75	The base of the ribosomal P stalk fromMethanococcus jannaschii: crystallization and preliminary X-ray studies. Acta Crystallographica Section F: Structural Biology Communications, 2013, 69, 1288-1290.	0.7	2
76	Crystallographic analysis of archaeal ribosomal protein L11. Acta Crystallographica Section F, Structural Biology Communications, 2015, 71, 1083-1087.	0.4	2
77	NMR and crystallographic structural studies of the Elongation factor P from Staphylococcus aureus. European Biophysics Journal, 2020, 49, 223-230.	1.2	2
78	The role of positive charged residue in the proton-transfer mechanism of two-domain laccase from <i>Streptomyces griseoflavus</i> Ac-993. Journal of Biomolecular Structure and Dynamics, 2022, 40, 8324-8331.	2.0	2
79	Crystal structure of a mutant of archaeal ribosomal protein L1 from Methanococcus jannaschii. Crystallography Reports, 2014, 59, 394-398.	0.1	1
80	Structural investigation of endoglucanase 2 from the filamentous fungus Penicillium verruculosum. Crystallography Reports, 2017, 62, 254-259.	0.1	1
81	The key role of E418 carboxyl group in the formation of Nt.BspD6I nickase active site: Structural and functional properties of Nt.BspD6I E418A mutant. Journal of Structural Biology, 2020, 210, 107508.	1.3	1
82	ls RsfS a Hibernation Factor or a Ribosome Biogenesis Factor?. Biochemistry (Moscow), 2022, 87, 500-510.	0.7	1
83	Crystallization of mutant forms of the \hat{I}^3 subunit of archaeal translation initiation factor 2. Crystallography Reports, 2014, 59, 71-74.	0.1	0
84	Preliminary X-ray diffraction study of crystals of photosystem II from Thermosynechococcus elongates. Crystallography Reports, 2014, 59, 75-77.	0.1	0
85	Three-dimensional structures of unligated uridine phosphorylase from Yersinia pseudotuberculosis at 1.4 Ã resolution and its complex with an antibacterial drug. Crystallography Reports, 2015, 60, 525-531.	0.1	0
86	Structure of a complex of uridine phosphorylase from Yersinia pseudotuberculosis with the modified bacteriostatic antibacterial drug determined by X-ray crystallography and computer analysis. Crystallography Reports, 2015, 60, 217-226.	0.1	0